Smart Structures and Systems, *Vol. 15, No. 3 (2015) 699-715*
DOI: http://dx.doi.org/10.12989/sss.2015.15.3.699

A statistical framework with stiffness proportional damage sensitive features for structural health monitoring

Luciana Balsamo, Suparno Mukhopadhyay and Raimondo Betti*

Department of Civil Engineering and Engineering Mechanics, Columbia University, New York, NY 10027, USA

(Received November 21, 2014, Revised January 27, 2015, Accepted February 5, 2015)

Abstract. A modal parameter based damage sensitive feature (DSF) is defined to mimic the relative change in any diagonal element of the stiffness matrix of a model of a structure. The damage assessment is performed in a statistical pattern recognition framework using empirical complementary cumulative distribution functions (ECCDFs) of the DSFs extracted from measured operational vibration response data. Methods are discussed to perform probabilistic structural health assessment with respect to the following questions: (a) "Is there a change in the current state of the structure compared to the baseline state?", (b) "Does the change indicate a localized stiffness reduction or increase?", with the latter representing a situation of retrofitting operations, and (c) "What is the severity of the change in a probabilistic sense?". To identify a range of normal structural variations due to environmental and operational conditions, lower and upper bound ECCDFs are used to define the baseline structural state. Such an approach attempts to decouple "non-damage" related variations from damage induced changes, and account for the *unknown* environmental/operational conditions of the current state. The damage assessment procedure is discussed using numerical simulations of ambient vibration testing of a bridge deck system, as well as shake table experimental data from a 4-story steel frame.

Keywords: stiffness proportional DSF; empirical complementary CDF; probabilistic damage detection

1. Introduction

Vibration based Structural Health Monitoring (SHM) usually involves either "model based" or "data based" techniques. In model based methods the parameters of an *assumed* analytical model of the true physical system are identified so that the response of the identified model mimics the measured response from the real structure (Friswell 2007). While the identification of an *accurate* parametric model of the structure will allow an *accurate* identification of the existence, location and severity of damage, *accurate* models of true physical systems are seldom available. Moreover, most model based approaches involve some nonlinear optimizations with only a limited number of model parameters to be optimized or identified. This requires a reliable *a priori* analytical model. If the representative model is not very reliable, applying conventional model based methods with all/most of the model parameters as unknowns may not converge to a unique solution (Katafygiotis and Beck 1998, Mukhopadhyay *et al*. 2014a, b).

*Corresponding author, Professor, E-mail: betti@civil.columbia.edu

http://www.techno-press.org/?journal=sss&subpage=8 ISSN: 1738-1584 (Print), 1738-1991 (Online)

Data-based methods rely exclusively on the data recorded from the true structure, and do not require an *a priori* definition of *accurate* physical models (Worden and Farrar 2013). Implemented in a statistical pattern recognition framework, they attempt to identify patterns of Damage Sensitive Features (DSFs) characterizing the structure's condition by analyzing its recorded vibration signatures. The DSFs extracted from the measured responses of a baseline structure are first used to construct a baseline statistical model of the DSFs (training phase), where the baseline structure represents the system in its present conditions. In the following, the baseline system is also referred to as the reference or healthy system, always implying that it represents a system under conditions that have been observed during the training phase. Subsequently, during the testing phase, the DSFs extracted from any new measured response of the structure are compared to the baseline statistical model to identify whether the structure is still in its reference conditions or has undergone any deterioration. Since measured data from different real damage states are not available, data-based SHM involves unsupervised learning, with any new measured data assigned to either the healthy class or a damaged class; questions on the type, location and severity of damage are usually left unanswered. Another challenge in data-based methods is the selection of an appropriate statistical model for the DSFs. The popular normal distribution assumption (Balsamo *et al*. 2014a) may not hold if the number of observations is small, e.g., when instrumentation and data storage/processing costs, faulty instruments etc. lead to small training data set.

In this paper, the comparative advantages of model-based and data-based techniques are combined to a "mixed" approach in vibration based SHM. Due to the intuitive relationship of modal properties to structural characteristics, a modal parameter based DSF may be expected to successfully locate and quantify damage. In fact, several studies have used modal parameters for damage detection (Kim and Stubbs 2003, Yuen *et al*. 2006, Duan *et al*. 2007, Balsamo *et al*. 2013a, b, Huang *et al.* 2012). While modal frequencies, being global features, may be relatively insensitive to local structural damage, mode shapes, being "spatially distributed" features, contain information which may be employed for damage localization (Farrar *et al*. 2001). However, the direct comparison of mode shapes using inner product norms, e.g., the Modal Assurance Criterion, may not provide sufficiently discernible results for structural damage detection, as the differences reflected by such measures are of a lower order than the differences in the structural flexibility matrix (Mukhopadhyay *et al*. 2012). Instead, in (Mukhopadhyay *et al*. 2012, Balsamo *et al*. 2013b) modal parameter comparative measures which mimic changes in the structural flexibility and stiffness matrices are derived. In this paper, we use a stiffness proportional DSF, which gives a measure of the relative difference between the corresponding diagonal elements of the stiffness matrices of two models at comparison. The DSF is defined in terms of experimentally identified modal parameters, which may be identified from the response of the monitored structural system using any modal analysis technique. We consider here the most feasible operational testing scenario (output-only data).

The damage assessment procedure is developed in the statistical pattern recognition paradigm using the DSFs extracted from measured response data. The Empirical Complementary Cumulative Distribution Functions (ECCDFs) of the extracted DSFs are computed, and damage assessment is performed by comparing the ECCDFs obtained during the testing stage with those created during the training stage. The proposed structural health assessment exercise attempts to answer the questions: (1) "Is there a change in the current state of the structure compared to the baseline state?", (2) "Does the change indicate a localized stiffness reduction or increase?", and (3) "What is the severity of the change in a probabilistic sense?". The possible scenario of localized stiffness increase is intended for applications in retrofitting operations (Nayeri *et al*. 2007).

It has been widely reported that modal parameters are significantly affected by “non-damage” related structural variations, induced, for example, by environmental/operational fluctuations (Sohn2007, Soyoz and Feng 2009). Such effects are taken into account here, using lower and upper bound ECCDFs, obtained from training response time histories measured in different environmental/operational conditions, to define the baseline structural state. Such an approach is intended to decouple normal structural variations from damage induced changes in the values of the proposed DSFs. The lower and upper bound baseline ECCDFs are also used to quantify the uncertainty in damage probability vs. damage severity curves, induced by *unknown* environmental/operational conditions in the testing phase.

The proposed SHM framework addresses several relevant issues. Defining a physically meaningful DSF in a model-based setting allows not only the detection of damage, but also its location and severity estimation. On the other hand, the data-based SHM strategy statistically tests for the existence of damage at any location, and expresses the damage severity through damage probability vs. severity curves, accounting for the different inevitable sources of uncertainty, including those induced by environmental/operational fluctuations. It is worth emphasizing that the proposed algorithm does not require the definition of reliable models describing the effects of environmental/operational conditions on structural parameters, nor does it require the measurements of any operational or environmental variable, e.g., temperature measurements. Hence, the proposed approach may be applied even in those scenarios where measurements of these external conditions are unavailable. While the DSF computation does not require *a priori* knowledge of the mass/stiffness parameter values, limiting the modeling assumptions only to the knowledge of the model class, the use of ECCDFs further avoids the assumption of any particular parametric distribution to statistically model the DSFs. Finally, in addition to damage detection, the proposed approach may also be used to validate retrofitting operations.

The DSF computation is discussed in Section 2. The derivation of the training and testing ECCDFs of the DSFs are discussed in Section 3, and the different levels of damage assessment are discussed in Section 4 using numerical simulations of ambient vibration testing of a bridge deck system. In Section 5, the approach is applied to shake table experimental data from a 4-story steel frame.

2. Stiffness proportional damage sensitive feature

In modeling structural damage as localized stiffness reduction, a DSF which is tailored to measure the deviation of stiffness properties from a baseline state should be ideal. To define such a DSF, consider an N degrees of freedom (DOF) classically damped model of a system, with $N\times N$ mass and stiffness matrices, respectively denoted by $\mathbf{M}$ and $\mathbf{K}$. Let the state of the system described by $\{\mathbf{M}, \mathbf{K}\}$ be the baseline state. Let an alternative state of the system, representing it in an unknown condition, be denoted by $\{\mathbf{M}^*,\mathbf{K}^*\}$. Then, the DSF discussed here measures the departure of the (i,i)th element of $\mathbf{K}^*$ from the (i,i)th element of $\mathbf{K}$

$$\mathrm{DSF}_i = \frac{K_{i,i} - K^*_{i,i}}{K_{i,i}}. \tag{1}$$

Since this DSF measures the relative change in the system's local stiffness properties, it is named *Stiffness Proportional Damage Sensitive Feature* (SPDSF). Since the DSFs discussed in this section are related to the different DOFs constituting the model of the system, these DSFs may be used not only to test for the existence of damage in the system, but also to locate the damage to the neighborhood of any particular DOF. Moreover, since the DSFs provide a measure of the relative change, with respect to the baseline state, in the diagonal elements of the stiffness matrix, they may also be used to assess the severity of any localized damage.

Let λ_j and $\boldsymbol{\phi}_j$ denote the jth eigenvalue and mode shape vector of the model corresponding to the baseline state, and ϕ_{ij} the ith component (corresponding to DOF i) of $\boldsymbol{\phi}_j$. Any appropriate operational modal analysis technique may be used to identify these parameters. In this paper we consider systems which can be represented through lumped mass models, i.e., $\mathbf{M}$ and $\mathbf{M}^*$ are diagonal. The DSF in Eq. (1) can then be written in terms of the modal parameters of the two states of the system as

$$\mathrm{DSF}_i = 1 - \frac{\alpha^*}{\alpha} \frac{\left(\sum_{j=1}^{N} \phi_{i,j}^2 \beta_j^{-1}\right)^2 \left(\sum_{j=1}^{N} \phi_{i,j}^{*2} \lambda_j^* \beta_j^{*-1}\right)}{\left(\sum_{j=1}^{N} \phi_{i,j}^{*2} \beta_j^{*-1}\right)^2 \left(\sum_{j=1}^{N} \phi_{i,j}^2 \lambda_j \beta_j^{-1}\right)} \tag{2}$$

with the superscript * denoting parameters belonging to the alternative $\{\mathbf{M}^*, \mathbf{K}^*\}$ state. In Eq. (2), the β factors $\{\beta_1 = 1, \beta_2, \ldots, \beta_N\}$ are *proportional* mass normalizing factors, which account for the arbitrary scaling of the identified mode shapes in output-only/base excitation situations, while the scalar α is the *true* mass normalizing factor for mode 1; for any mode j, $\alpha\beta_j$ is the *true* mass normalizing factor. In tests with known input forces, with one collocated sensor-actuator pair, it is possible to directly identify the mass normalized mode shapes (e.g., Mukhopadhyay 2014a), and so the α and all β's in Eq. (2) become equal to 1. However, when considering the more feasible output-only/base excitation scenarios, these factors need to be estimated separately. The first factor β_1 is taken as 1, since in output-only situations, for models with diagonal $\mathbf{M}$, one can identify only a model *proportional* to the true model by a single scalar factor without using any *a priori* knowledge of the value of any physical parameter (Mukhopadhyay 2014b). The remaining $(N - 1)$ unknown β_j's may be obtained by imposing any known topological requirements of the $\mathbf{M}$ and $\mathbf{K}$ matrices (Mukhopadhyay 2014b). Imposing the sparsity requirement of a diagonal $\mathbf{M}$, one gets the following linear system of equations whose least squares solution gives the unknown β_j's

$$\sum_{j=2}^{N} \phi_{i,j}\phi_{l,j} / \beta_j = -\phi_{i,1}\phi_{l,1} \qquad \forall\, i, l \in S \text{ and } i \neq l \tag{3}$$

where S is the set of instrumented DOFs (a subset of all the N DOFs), where the output responses are measured. One can similarly obtain a least squares solution for the factors of the alternative system. To evaluate the ratio α^*/α, one would need some assumption on the value of any physical parameter of the system. Assuming that the change in the total mass (= sum of all element masses) of the system in its transition from one state to another is minimum, this ratio may be estimated as

$$\frac{\alpha^*}{\alpha} = \frac{\sum_{i=1}^{N}\left(\sum_{j=1}^{N} \phi_{i,j}^2 \beta_j^{-1}\right)}{\sum_{i=1}^{N}\left(\sum_{j=1}^{N} \phi_{i,j}^{*2} \beta_j^{*-1}\right)} \tag{4}$$

If the system is instrumented with N_s sensors, Eq. (3) will represent $N_s(N_s - 1)/2$ equations, leading to the minimal instrumentation requirement of $N_s \geq [1 + \sqrt{(8N - 7)}]/2$ for estimation of all the $(N - 1)$ β_j's. Even though the DSF in Eq. (2) is written for an identified complete spectrum, in situations where only $N_m<N$ modes are identified from the data, the DSF may still be computed using only these N_m modes in the summation. However, in order to identify the normalizing factors through Eq. (3), all N modes need to be identified at the sensors locations; if $N_m<N$ modes are identified, then other approaches (e.g., Parloo *et al*. 2002) may be used to compute the corresponding β factors.

3. Empirical complementary cumulative distributions of SPDSF

Unlike traditional DSFs, which represent a single state of the system, inherent in the definition of the DSFs in Section 2 is a comparison between two states of the system. For example, a change in the stiffness of an element connecting nodes i and l would be reflected in a change in the values of the ith and lth elements in the main diagonal of $\mathbf{K}$, and this change would be captured by DSF_i and DSF_l. However, these DSFs, being dependent on the identified frequencies and mode shapes, will not only measure the change in the stiffness properties induced by structural damage, but will also measure stiffness changes induced by environmental and operational variability. Hence, it is pertinent that the damage detection procedure be able to distinguish between damage induced and non-damage induced fluctuations in the DSFs, so as to reduce instances of *false alarms* and *false safety*. This requirement defines an objective of the training phase: to define boundaries for the fluctuations of the DSFs that can be considered normal, and thereby define a reference zone against which new realizations of the DSFs, extracted from the system under unknown conditions, can be compared. To this end, we use the cumulative distribution functions (CDFs) of the DSFs, treating each DSF as a random variable.

The SHM problem can be cast in a probabilistic framework by introducing the "probability of damage" assigned to any model parameter (Yuen *et al*. 2006). Such a probability can be assigned to each diagonal element of $\mathbf{K}$, and be defined as the probability that the (i,i)th element of $\mathbf{K}^*$ be less than a prescribed fraction of the (i,i)th element of $\mathbf{K}$

$$P_i^{\text{damage}}(d) = P(K^*_{i,i} < (1-d)K_{i,i}) \tag{5}$$

where d is the fractional stiffness reduction (damage). Eq. (5) can be rewritten using Eq. (2) as

$$P_i^{\text{damage}}(d) = P\left(\frac{K_{i,i} - K^*_{i,i}}{K_{i,i}} > d\right) = 1 - P\left(\frac{K_{i,i} - K^*_{i,i}}{K_{i,i}} < d\right) = 1 - \mathrm{CDF}_{\mathrm{DSF}_i}(d) \tag{6}$$

The training procedure to build statistical models of the baseline state DSFs, encompassing the normal variability of the CDFs of the DSFs, can then be performed as discussed herein. Let n_{tr} denote the number of measurement campaigns (i.e., number of sets of measured response data) that have been conducted on the monitored system under *different healthy conditions*; these *different healthy conditions* include different environmental and operational conditions of the healthy state of the system. With N_s sensors, located at the DOFs in $\mathcal{S}$, in each measurement campaign, a set $\mathrm{Y} = \{\mathbf{\Lambda}^p, \mathbf{\Phi}^p\}$, for $p = 1, \dots, n_{\text{tr}}$, of modal parameters may be identified, where $\mathbf{\Lambda}^p$ and $\mathbf{\Phi}^p$ respectively contain the N eigenvalues and mode shapes at the N_s measured DOFs identified from the pth set of measured response data. The set Y is then divided into two subsets $\mathrm{Y_H}$ and $\mathrm{Y_V}$ such that

$$\mathrm{Y_H} \cup \mathrm{Y_V} = \mathrm{Y}; \quad \mathrm{Y_H} \cap \mathrm{Y_V} = \varnothing; \quad \mathrm{Y_H}, \mathrm{Y_V} \neq \varnothing; \quad |\mathrm{Y_H}| = n_H; \quad |\mathrm{Y_V}| = n_V \tag{7}$$

Now, the modal parameters in $\mathrm{Y_H}$ are considered as reference, while those in $\mathrm{Y_V}$ are considered to come from an unknown state of the system, i.e., following the terminology used in Section 2, $\mathrm{Y_H}$ is treated as the set of modal characteristics identified from baseline states, while $\mathrm{Y_V}$ is treated as the set of modal properties identified from the system under unknown conditions. Then, each set of modal parameters in $\mathrm{Y_V}$ is compared with each and every set of modal parameters in $\mathrm{Y_H}$ using the DSF of Eq. (2); this results in a total of n_V sets DSF_i, $\forall i \in \boldsymbol{S}$, each set containing n_H values. Empirical Cumulative Distribution Functions (ECDFs) of DSF_i are then computed using Eq. (8) (Hanselmann *et al.* 2007), for each of these n_V sets, treating the n_H DSF_i values in each set as random realizations

$$\mathrm{ECDF}_{DSF_i}^{j}(d) = \frac{1}{n_H} \sum_{p=1}^{n_H} U(d - DSF_i^{p,j}) \qquad \forall\ j = 1,..., n_V \tag{8}$$

where $U(z)$ is the Heaviside function: $U(z) = \{0, 0.5, 1\}$ for $z\{<, =, >\}$ 0. Eq. (8) is evaluated over a set of d values such that the computed ECDF(d)'s range from 0 to 1. $\mathrm{ECDF}_{DSF_i}^{j}(d)$ in Eq. (8) can be substituted in place of $\mathrm{CDF}_{DSF_i}(d)$ in Eq. (6); the resulting $P_i^{\mathrm{damage}}(d)$ in Eq. (6), computed as $1 - \mathrm{ECDF}_{DSF_i}(d)$, is then referred to as the *Empirical Complementary Cumulative Distribution Function* (ECCDF) of DSF_i. In this way, we get n_V curves representing $\mathrm{ECDF}_{DSF_i}(d)$, one for each data set in $\mathrm{Y_V}$. The maximum and minimum bounds of these n_V number of $\mathrm{ECCDF}_{DSF_i}(d)$ are then computed, to estimate an acceptable range of d, denoting normal environmental/operational variability, and also to get lower and upper bound exceedance probabilities, given by the lower and upper bound ECCDFs, associated with each value of d in this range, for each DSF_i. At the time of testing, a new set of response data is measured with the N_s sensors from the structure under unknown conditions, and a single set of modal parameters is identified from this data. This new set of modal parameters is compared, using Eq. (2), to each of the n_H sets of parameters in $\mathrm{Y_H}$ obtained during the training stage. The resulting n_H values of DSF_i are then used to compute a single $\mathrm{ECCDF}_{DSF_i}(d)$ following the same procedure as in the training stage. This single $\mathrm{ECCDF}_{DSF_i}(d)$ is then compared with the lower and upper bounds of $\mathrm{ECCDF}_{DSF_i}(d)$ obtained in the training stage for damage assessment. This comparison may be performed using different measures, as discussed in the next section with a numerical example.

4. Different levels of damage assessment with numerical example

4.1 Numerical example

To test the validity of the proposed approach and to further define the procedures to identify, locate and define the extent of damage, we consider the simple lumped mass model of a bridge deck of Fig. 1. The model consists of 12 lumped masses and 20 flexural links, and is assumed to vibrate along the z direction. The energy dissipation characteristics of the system are modeled through proportional damping, by assigning 1% damping ratio to each mode.

Table 1 lists the 10 different states considered here. States U1 to U5 represent different healthy conditions: for example, state U2 may represent a scenario where only the –*y* side of the bridge deck is subjected to a temperature increase, while state U5 corresponds to a state where only the +*y* side of the deck is subjected to temperature decrease. States D1 to D4 represent different damage scenarios, with local damages defined with respect to different undamaged states, as may be expected in practice. State R1 represents the condition where a portion of the –*y* girder is retrofitted.

To construct the training data sets, 50 tests are simulated on each of the five healthy states. Therefore, the set Y defined in Section 3 consists of 250 data sets. For a given test *r*, the value of the *i*th stiffness parameter, $k_i^{(r)}$, is chosen as $k_i^{\mathrm{U}m} + U(-0.01, 0.01)k_i^{\mathrm{U}m}$, where $k_i^{\mathrm{U}m}$ is the mean value of the flexural stiffness k_i for the undamaged scenario U*m*, *m*=1,…,5 (Table 1), and $U(-0.01, 0.01)$ is the uniform probability distribution between the limits – 0.01 and 0.01. The variability of the stiffness parameters depicted in Table 1 is adopted to model systematic changes induced, for instance, by environmental effects, while the variability induced by the perturbation obtained via $U(-0.01, 0.01)$ is used to mimic the effects of operational and modeling assumptions. The ± 0.01 limits are used as an example, but any range of values producing moderate changes to the structural properties would be similarly acceptable. It should be emphasized that, with the simulated environmental and operational variability, any $(i,i)^{\mathrm{th}}$ element of the healthy stiffness matrix has an approximately ±1.7% variability with respect to the baseline state, which is of the same order as the damage/retrofit induced mean changes (– 5% in states D2 and D4, +8.3% in R1,– 6.6% in D1 and D3); moreover, the difference between the stiffest and the most flexible healthy structure in terms of any $(i,i)^{\mathrm{th}}$ element of the stiffness matrix (approximately 3.3%) is higher than the difference between the most flexible healthy structure and the most stiff damaged structure (approximately 2.4%), thereby including the possibility of damage being masked by environmental/operational variability. Since such a possibility poses a pressing and relevant concern in SHM applications, the performance of the proposed approach is evaluated under such conditions.

Each of the 250 sets of healthy structural parameters is used to simulate the response of the system to Gaussian white noise input force applied at all the DOFs. The resulting response accelerations are corrupted by adding 10% root mean square Gaussian white noise sequences, to represent measurement noise. In this example, only the response accelerations measured at DOFs 4 to 9, 11 and 12 are considered, to represent a partial instrumentation set-up. The set of 250 "measured" acceleration time histories is used to identify the modal frequencies and arbitrarily scaled mode shape components at the instrumented DOFs. In this numerical example, a stochastic subspace identification algorithm is used for this purpose, namely the Enhanced Canonical Correlation Analysis (ECCA) (Hong *et al*. 2013). The 250 sets of identified modal properties are then divided into the subsets $\mathrm{Y_H}$ and $\mathrm{Y_V}$, each of cardinality 125 (n_H and n_V are both equal to 125), both containing 25 realizations from each of the 5 undamaged scenarios. The methods discussed in Sections 2 and 3 are then employed to derive the SPDSFs for the instrumented degrees of freedom and the boundaries of the ECCDFs.

To construct the testing ensemble, 30 tests are performed on each of the 10 states of Table 1, and the structural response is simulated adopting the same procedure used to construct the training data sample. The modal parameters identified through ECCA from each testing data set are compared to the n_H sets of training modal parameters in $\mathrm{Y_H}$, and the resulting testing ECCDF at each measured DOF is constructed.

Fig. 2 compares the 30 *testing* ECCDFs (thin black curves) in states U1, D1 and R1 with the lower (dashed thick line) and upper (continuous thick line) bound *training* ECCDFs for DSF_6. It may be noted that while the ECCDFs obtained from State U1 are contained within the training boundaries, the testing ECCDFs from State D1 are shifted to the right beyond the upper bound, indicating damage occurrence in one of the elements connected to mass 6 (see Table 1). On the contrary, the testing ECCDFs from State R1 are shifted to the left of the lower bound, validating a retrofitting operation to a portion of the structure in the proximity of sensor 6. Within a deterministic framework, a value of the SPDSF greater than 0 would indicate damage, as only one healthy state would be considered, and would have thus signaled the presence of damage in many of the tests performed on state U1. On the contrary, the initial training phase performed in the currently proposed approach enables us to set a reasonable range of values of *d*, within which the observation of a non-zero *d* can be attributed to the influence of external factors, e.g., temperature, traffic, wind, etc.

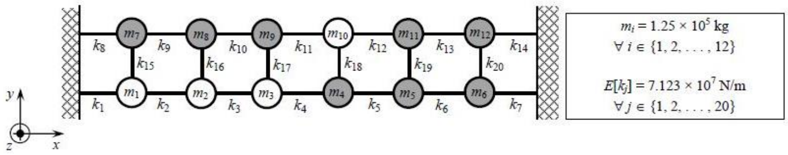

Fig. 1 Bridge model and baseline parameters used in numerical example. Shaded lumped masses denote sensor locations in a partial instrumentation setup.

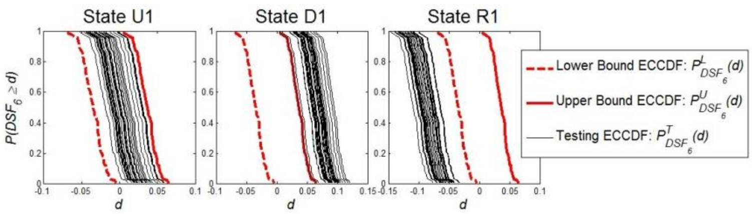

Fig. 2 ECCDFs of SPDSFs at DOF 6 under States U1, D1 and R1

Table 1 Different states of the bridge deck model considered for the numerical example

State	Condition	Description	Affected DOFs
U1	Undamaged	$k_i^{U1} = \mathrm{E}[k_i]\ \forall\, i \in \{1,\ldots,20\}$	-
U2	Undamaged	$k_i^{U2} = 0.99\,\mathrm{E}[k_i]\ \forall\, i \in \{1,\ldots,7\}$	1-6
U3	Undamaged	$k_i^{U3} = 1.01\,\mathrm{E}[k_i]\ \forall\, i \in \{1,\ldots,7\}$	1-6
U4	Undamaged	$k_i^{U4} = 0.99\,\mathrm{E}[k_i]\ \forall\, i \in \{8,\ldots,14\}$	7-12
U5	Undamaged	$k_i^{U5} = 1.01\,\mathrm{E}[k_i]\ \forall\, i \in \{8,\ldots,14\}$	7-12
D1	Damaged	$k_6^{D1} = 0.80 k_6^{U1}$	5 and 6
D2	Damaged	$k_6^{D2} = 0.85 k_6^{U2}$	5 and 6
D3	Damaged	$k_{18}^{D3} = 0.80 k_{18}^{U3}$	4 and 10
D4	Damaged	$k_{18}^{D4} = 0.85 k_{18}^{U4}$	4and 10
R1	Retrofitted	$k_6^{R1} = 1.25 k_6^{U5}$	5 and 6

4.2 Damage/retrofit detection and location

In order to identify damage occurrence/retrofitting at a given location, it is necessary to compare the testing ECCDFs with the training boundaries. To fulfill this task, we explore here the use of the Lukaszyk-Karmowski metric (Lukaszyk 2004), which compares two probability distributions as

$$D_{Y,X} = D_{X,Y} = \int_{-\infty}^{+\infty}\int_{-\infty}^{+\infty} | x - y | \, f_X(x) g_Y(y) \, \mathrm{d}x \, \mathrm{d}y \tag{9}$$

where $f_X(x)$ and $g_Y(y)$ are the probability density functions of the random variables *x* and y. $D_{X,Y}$ is not a distance metric in the strict sense, as $D_{X,X}$ is equal to 0 only if *x* is an exact value. The property of the Lukaszyk-Karmowski metric that makes it appealing from our perspective is that it satisfies the triangle inequality as an equality: $D_{X,Z} = D_{X,Y} + D_{Y,Z}$. This property may be exploited as follows: let $f_L(d_L)$, $f_U(d_U)$, and $f_T(d_T)$ be the empirical probability density functions (epdfs) corresponding to the lower training bound, the upper training bound and the testing set of SPDSFs, respectively. Then, for example, when the testing ECCDF is obtained from data collected on the structure under undamaged conditions, the Lukaszyk-Karmowski distance of the lower training bound from the upper one satisfies the following relation

$$D_{L,U} = \int_{-\infty}^{+\infty}\int_{-\infty}^{+\infty} | d_L - d_U | \, f_L(d_L) f_U(d_U) \, \mathrm{d}d_L \, \mathrm{d}d_U = D_{L,T} + D_{T,U} \Rightarrow \frac{D_{L,U}}{D_{L,T} + D_{T,U}} \approx 1 \tag{11}$$

Similar relations hold when the system is damaged or retrofitted (Eqs. (12))

$$\frac{D_{L,T}}{D_{L,U} + D_{U,T}} \approx 1 \rightarrow \textbf{Damage} \; ; \; \frac{D_{U,T}}{D_{L,U} + D_{L,T}} \approx 1 \rightarrow \textbf{Retrofit} \tag{12}$$

In Eqs. (11) and (12) we use $\approx$ to account for numerical errors introduced in the computation of the epdf from the ECCDF, and in the 2-D numerical integration necessary to compute the Lukaszyk-Karmowski metric, which in this paper is performed employing trapezoidal rule.

Table 2 lists the results obtained by employing the said metric to detect and locate damage. In Table 2, for each state, the ratio n/30 indicates the number of tests, n, for which a change in the given diagonal term of the stiffness matrix is identified; the letter in parenthesis indicates whether that change is identified as due to damage (D) or retrofitting (R). Evidently, using said metric it is possible to correctly identify damage between degrees of freedom 5 and 6 (States D1 and D2), and damage around degree of freedom 4 (States D3 and D4), with reasonable accuracy. When dealing with damage scenarios D3 and D4 the detailed estimation of damage location is not possible, owing to incomplete instrumentation, specifically due to the absence of sensors at DOFs 3 and 10. Hence, for such states, we are only able to detect damage around DOF 4, but unable to exactly locate the damaged element. Note, however, that owing to the testing ECCDFs at DOF 5 falling within the training bounds, we can say k_5 is not one of the damaged elements, so that States 3 and 4 would be identified as damage scenarios where damage occurred on element(s) k_4 and /or k_{18}.

In this example, Type II error, i.e. the percentage of damaged instances incorrectly identified as undamaged, is equal to 12.78% (23 out of 180 cases), and it is almost entirely due to missed damage identification of the milder damage conditions (States D2 and D4). Type I error, i.e. the incorrect identification of an undamaged state as damaged, is much lower and equal to 0.81% (18 out of 2220 cases). The retrofitting operation is correctly validated, with 100% accuracy, between degrees of freedom 5 and 6. The percentage of tests erroneously concluding that a certain area of the system has been retrofitted is 0.56% (13 out of 2340 cases). However, this latter error is of little concern, as the approach here proposed would be used only to verify that a given area of the system has been actually retrofitted. In practice, the retrofitted area is known *a priori*, and the use of the proposed structural health monitoring technique would only validate such an operation. An indication of retrofitting in a non-retrofitted area should be then judged as merely due to testing conditions slightly dissimilar to those attained during training.

4.3 Stiffness change severity assessment

Once changes in stiffness have been identified, it is important to quantify the extent of such changes to conclude whether the identified increase/decrease of the stiffness property is due to an actual change in the structural characteristics or is only due to healthy conditions slightly different from those learnt during training.

At this point, it is important to emphasize the key premise the proposed structural health monitoring strategy is based on. In fact, it is recognized that thinking of the healthy system as represented by a single configuration of the structure is probably inappropriate, but it is rather more realistic to consider the healthy state as a variety of possible conditions where the structural properties might slightly change without leading the structure to perform differently from how it was originally designed. While by itself the testing ECCDF, here onwards denoted as $P^T_{DSF_i}(d)$, gives a probabilistic representation of the damage severity, this representation does not account for the inherent variability in the healthy system's ECCDFs. Hence, the damage severity obtained only using $P^T_{DSF_i}(d)$ may over/underestimate the actual damage severity. To account for the healthy system variability, the lower and upper training ECCDFs, denoted as $P^L_{DSF_i}(d)$ and $P^U_{DSF_i}(d)$ respectively, can be exploited as follows. We select a certain percentile from $P^L_{DSF_i}(d)$, α_L, and another from $P^U_{DSF_i}(d)$, α_U. The values of the stiffness change magnitude, d, corresponding to α_L and α_U should define a *reasonable* range of healthy system's variability, i.e., a range which excludes extreme variations of the healthy system. Since $P^L_{DSF_i}(d)$ and $P^U_{DSF_i}(d)$ correspond respectively to the stiffest and softest healthy systems, such a reasonable range for d should correspond to a lower percentile from $P^L_{DSF_i}(d)$ and a higher percentile of $P^U_{DSF_i}(d)$. Reasonable values for α_L would range between 1 and 5, while for α_U between 95 and 99, since such values conform to low and high percentiles, corresponding to a very stiff and a very soft healthy condition, respectively. Here we select α_L equal to 5, and α_U equal to 95. Hence, we subtract the bound defined by the 5th percentile of $P^L_{DSF_i}(d)$, $d_L^{5\%}$, and the 95th percentile from $P^U_{DSF_i}(d)$, $d_U^{95\%}$ (Fig. 3(a)) from the testing d's: the resulting first ECCDF, $P^{LT}_{DSF_i^S}(d^S)$, gives the exceedance probabilities of damage with respect to the stiffest healthy condition, while the second, $P^{UT}_{DSF_i^S}(d^S)$, quantifies the exceedance probability vs. the damage extent with respect to the softest healthy condition.

Table 2 Results for stiffness change occurrence identification and location

State	$K_{4,4}$	$K_{5,5}$	$K_{6,6}$	$K_{7,7}$	$K_{8,8}$	$K_{9,9}$	$K_{11,11}$	$K_{12,12}$
U1	***1/30 (D)***	0/30	***1/30 (R)***	0/30	0/30	0/30	***1/30 (R)***	***3/30 (D)***
U2	0/30	***1/30 (D)***	***1/30 (D)***	0/30	0/30	***1/30 (D)***	0/30	0/30
U3	***1/30 (R)***	0/30	***1/30 (D)*** ***1/30 (R)***	***1/30 (R)***	0/30	0/30	***1/30 (D)***	***2/30 (D)***
U4	0/30	0/30	***1/30 (D)***	0/30	0/30	0/30	***1/30 (D)*** ***1/30 (R)***	0/30
U5	0/30	0/30	0/30	0/30	0/30	0/30	***1/30 (R)***	0/30
D1	0/30	***29/30 (D)***	***29/30 (D)***	0/30	***1/30 (R)***	0/30	***1/30 (R)***	0/30
D2	0/30	***27/30 (D)***	***20/30 (D)***	0/30	0/30	0/30	***1/30 (D)*** ***1/30 (R)***	0/30
D3	***30/30 (D)***	0/30	0/30	0/30	0/30	0/30	***1/30 (D)***	0/30
D4	***22/30 (D)***	0/30	0/30	0/30	0/30	0/30	0/30	0/30
R1	***1/30 (R)***	***30/30 (R)***	***30/30 (R)***	***2/30 (R)***	0/30	0/30	0/30	***3/30 (D)***

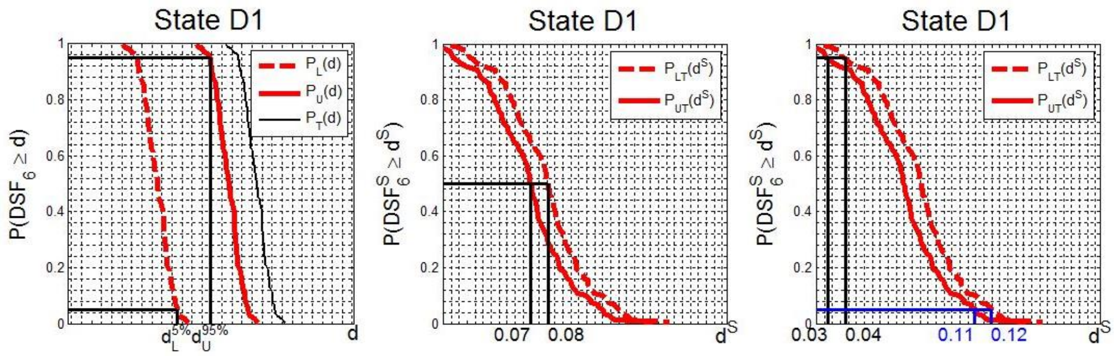

(a) (b) (c)

(a) Definition of $d_L^{5\%}$ and $d_U^{95\%}$, (b) Estimation of damage severity (median) and (c) Estimation of damage severity (5th and 95th percentiles)

Fig. 3 Estimation of damage severity

Fig. 3(b) shows the ECCDFs obtained for a test under state D1 at DOF 6. In Figs. 3(b) and 3(c), the ordinate and abscissa labels display DSF^S and d^S in place of DSF and d, respectively, to emphasize that the values of the random variable are not those evaluated during testing, but those obtained by subtracting $d_U^{95\%}$ and $d_L^{5\%}$ from the testing values. The median amount of damage extent with respect to the stiffest healthy condition is equal to 0.08 (dashed thick red line in Fig. 3(b)), while with respect to the softest healthy state is equal to 0.07 (continuous thick red line in Fig. 3(b)). From the previous results, we know that the element between DOFs 5 and 6 is damaged; if we assume that all spring elements connected to mass 6 have the same stiffness values, we can then estimate the amount of remaining stiffness, γ, of element k_6 according to Eq. (14):

$$P(DSF_6 > d) = P\left(1 - \frac{k_6^* + k_7^* + k_{20}^*}{k_6 + k_7 + k_{20}} > d\right) = P\left(1 - \frac{2k + \gamma k}{3k} > d\right) = P(\gamma < 1 - 3d). \tag{14}$$

It is important to note that, to perform damage severity assessment as in Eq. (14), one needs to know which are the stiffness elements connecting to the node under consideration, i.e., one needs to know the model class representing the system, which is a common assumption in most SHM techniques attempting to quantify damage severity. Using Eq. (14), it is possible to conclude that, under the damage scenario D1, there is 50% probability that the remaining stiffness of the damaged element between DOFs 5 and 6 be less than 0.79(= 1 - 3d = 1 - 3×0.07) when compared to the softest healthy system, and 0.76 (= 1 - 3×0.08) when compared to the stiffest healthy system (see Fig. 3(b)). Moreover, exploiting the 5th and 95th percentile of the ECCDFs of Fig. 3(c), it is possible to assess that there is only 5% probability that the remaining stiffness is lower than 0.67, but 95% probability that is lower than 0.91, with respect to the softest system. On the other hand, when considering the stiffest healthy condition, there is only 5% probability that the remaining stiffness of k_6 be lower than 0.64, but 95% probability that be lower 0.88. Since the actual range of variability of the simulated k_6 is within 0.73 and 0.82, the damage extent estimates are assumed to be reasonably accurate. Performing the same approach for all other tests under damaged cases D1 and D2, and retrofitted case R1, the results are equally accurate. As mentioned in section 4.2, owing to partial instrumentation, it is not possible to estimate with comparable accuracy the damage extent for damage states D3 and D4. If we assume that both elements k_4 and k_{18} are damaged and that the healthy counterparts share the same stiffness values, the stiffness retention of the two elements would range between 0.955 and 0.94; on the contrary, if we assume that only one element is damaged, values similar to those given for the state D1 are obtained.

5. Shake table experımental applıcatıon

For the experimental application of the proposed SHM approach, a 4-story singlebay laboratory scale A36 steel frame structural model is considered (Fig. 4).The frame has an inter-story height of 533 mm, floor plate dimensions of 610 x 457 x 12.7 mm, and it is diagonally braced in one direction (North-South direction), from here onwards denoted as the strong direction, as opposed to the perpendicular direction (East-West direction), referred to as the weak direction. The columns and the diagonal braces have cross-sectional dimensions of 50.8 x 9.5mm and 50.8 x 6.4 mm, respectively. All the structural connections are bolted using connection plates and angles. The frame is excited along the weak direction of bending. The base excitation is provided using the 1.5 x 1.5 m platform uniaxial hydraulic shaking table facility available at the Carleton Laboratory of Columbia University, New York. The frame is mounted on the table and the structure-table connection is sufficiently bolted to reproduce a fixed-base behavior. The frame is instrumented with 8 piezoelectric accelerometers, located at the plate levels on the column to plate connections, measuring the acceleration along the weak direction of bending (Fig. 4).The sampling rate of all instruments is at least 200 Hz for all the experiments considered herein. In the ensuing discussion, we use the structural acceleration at the centroids of the floors, referred to as $\ddot{u}_i$ in the following, for i= 1,…,4, obtained by averaging the recorded acceleration time histories: $\ddot{u}_1$= (A1 + A8)/2, $\ddot{u}_2$= (A2 + A7)/2, $\ddot{u}_3$= (A3 + A6)/2 and $\ddot{u}_4$= (A4 + A5)/2. Using the assumption of rigid floors and the coincidence of floor centers of mass and centroids, the frame is modeled as a 1-D 4-DOF system. Six different types of input ground motions (band limited white noise, Eurocode 8 compatible, El

Centro, Hachinohe, Kobe and Northridge) are applied to the table. For this application, the OKID/ERA (Luş et al. 1999) algorithm is employed to identify the modal properties of the frame, by using the measured acceleration responses of the floors as outputs and of the table as input.

To assess the applicability of the approaches discussed herein, in addition to the above frame, here onwards referred to as the "healthy" system (U1), an additional healthy condition U2 is considered, by adding two masses at the third floor: one on the south and the other on the north floor edge. The training data set is constituted by 89 input-output sets of acceleration histories. Four different "damaged" frames (D1 to D4) are also tested using the same set of 6 inputs. In these damaged frames, structural damage is simulated as stiffness reduction, by replacing one or more columns of the "healthy" frame with columns of reduced cross-sectional area (50.8 x 7 mm). The testing set consists of 144 data sets: 10 from state U1, 14 from state U2 and 30 from each of the four damaged states. The results of the stiffness change detection and location are presented in Table 4, using the same notation used to present the results for the numerical example. Type I error is again low and equal to 1.6% (5 out of 306 cases). Adversely, Type II error is equal to 25.6% (69 out of 270 cases). In fact, while damage scenarios D2 and D3 are correctly identified and located with 100% accuracy, the method identifies the stiffness change at DOF 3, but fails at identifying such change at DOF 2 for the damage scenario D1; similarly, for state D4, stiffness change at the third inter-story is identified both at DOF 3 and 2, but the stiffness reduction at the second inter-story cannot be identified from these results. One possible reason behind this misidentification is that both damage scenarios D1 and D3 cause torsion in the system, which may not be captured well by the 4 DOFs 1-D model used. Nonetheless, even in these scenarios the overall system is identified as damaged, and the region containing the damaged elements is identified accurately as well.

Fig. 5 shows the results of the stiffness change extent quantification. For any DOF, the plot in Fig. 5 is obtained as follows. Let $d_U^{95\%}$ correspond to the 95th percentile from the upper bound training ECCDF. Such $d_U^{95\%}$ is subtracted from the *d*'s associated with the 144 testing ECCDFs. From the resulting new shifted 144 ECCDFs, the median *d* values, here onwards referred to as $d_{UT}^{50\%}$, are obtained. Finally, for any given state, the average of such $d_{UT}^{50\%}$ values are computed over all the tests performed on that state, e.g. over the 10 tests on State U1. Comparing the average estimated damage extent displayed in Fig. 5 with the theoretical values presented in the last column of Table 3, it is evident that the proposed approach is able to quantify the extent of stiffness change with reasonable accuracy.

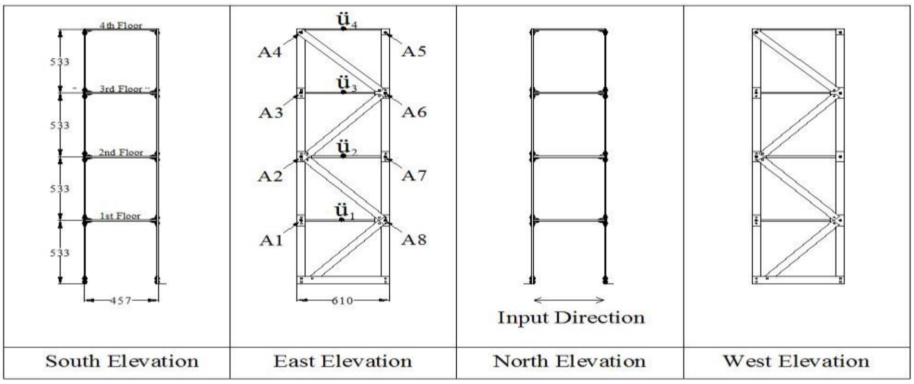

Fig. 4 Elevation views of the steel frame employed in the experimental application. Dimensions are in mm

Table 3 Different states of the steel frame considered for the experimental application

State	Condition	Description	Affected DOFs	Stiffness Reduction at affected DOFs
U1	Undamaged	Baseline condition	-	-
U2	Undamaged	40% mass addition to 3rd floor	-	-
D1	Damaged	15% stiffness reduction at 3rd floor	2 and 3	7.5% at DOFs 2 and 3
D2	Damaged	30% stiffness reduction at 3rd floor	2 and 3	15% at DOFs 2 and 3
D3	Damaged	60% stiffness reduction at 3rd floor	2 and 3	30% at DOFs 2 and 3
D4	Damaged	15% stiffness reduction at 2nd and 3rd floor	1, 2 and 3	7.5% at DOFs 1 and 3, 15% at DOFs 2

Table 4 Results for stiffness change identification and location

State	$\mathbf{K_{1,1}}$	$\mathbf{K_{2,2}}$	$\mathbf{K_{3,3}}$	$\mathbf{K_{4,4}}$
U1	***2/10 (D)***	0/10	***2/10 (R)***	***1/10 (D)*** ***2/10 (R)***
U2	0/14	0/14	0/14	0/14
D1	0/30	0/30	***30/30 (D)***	***2/30 (D)***
D2	0/30	***30/30 (D)***	***30/30 (D)***	0/30
D3	***17/30 (R)***	***30/30 (D)***	***30/30 (D)***	0/30
D4	0/30	***21/30 (D)***	***30/30 (D)***	0/30

An interesting observation from this experiment is the apparent increase in first-story stiffness with damage. The phenomenon may be appreciated in Table 4: at DOF1, for State D3, 17 out of the 30 tests identify an unexpected, systematic increase in stiffness at the first interstory. This is also observed in Fig. 5, which illustrates the estimated stiffness change extents in the different tested states. Such increase in stiffness is less marked for state D4, since the DOF 1 in this state also includes the effect of a damage in the second story; in fact, the average value of the estimated damage extent should be approximately equal to 0.075 in state D4 (Table 3). One possible explanation of the first story stiffness increase may be the activation of some strengthening mechanism (e.g., increased participation of the braces in load resistance, particularly strong torsional component, etc.) in the first story when there is damage at some other story. Such trend is more marked as the damage severity increases. In fact, while for damage scenarios D1 and D2 the average stiffness increase at the first interstory ranges between 4 and 6% (Fig. 5), for damage scenario D3 the increase in stiffness is nearly equal to 8%. This increase of the first interstory stiffness causes more than half of the tests performed on the frame under state D3 to be declared retrofitted at the first inter-story (Table 4). A similar unexpected increase in stiffness has been observed for the same structure also in (Fraraccio *et al.* 2008) where the stiffness properties of the frame structure have been identified using different approaches than the one presented in this paper.

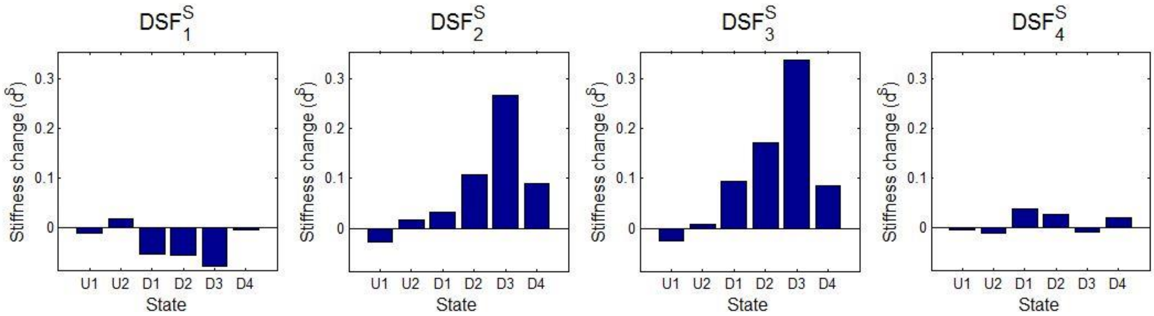

Fig. 5 Average damage extent for the six states of the experimental application

6. Conclusions

In this paper, a “mixed” approach for SHM using operational vibration response measurements is proposed. The DSFs, defined in a model based setting in terms of experimentally identified modal parameters, attempt to measure relative localized stiffness reductions. The health assessment is performed in a statistical pattern recognition framework using the DSFs extracted from response measurements. The features in the training stage, extracted from response measurements on the baseline structure in a wide variety of environmental/operational conditions, are used to compute a range of ECCDFs, from which lower and upper bound training ECCDFs are estimated. Such a training procedure intends to decouple the normal structural variations from damage induced changes, by defining a zone of normal variability of the baseline state through the estimated lower and upper bound training ECCDFs. The ECCDFs of DSFs extracted from the data collected in the testing stage are then compared against the lower and upper bound training ECCDFs to assess the presence, location and severity of any change in the structural stiffness parameters. To detect the existence of a stiffness change a method based on the Lukaszyk-Karmowski metric is exploited, which allows the user to also validate retrofitting operations. The results of a numerical example of ambient vibration testing of a bridge deck system illustrate that, with the localized definition of the DSF, using the aforementioned method, one may detect and locate the existence of any stiffness change with reasonable accuracy. After the existence and location of change detection, the severity of the change is also estimated using the testing and lower and upper bound training ECCDFs. The testing ECCDF is adjusted using different percentiles of the two training ECCDF bounds, resulting in a probability box model to represent the exceedance probability for different stiffness change severity levels. Such a model constitutes of a lower and an upper bound change probability vs. change severity curves, using which, for any given change severity, a lower and upper bound of the probability of exceedance can be estimated, and vice versa. The numerical example of the bridge deck shows that the severity of stiffness reduction/increase induced by damage/retrofitting may be estimated with reasonable accuracy using such curves. The two level uncertainty in the damage severity attempts to segregate: (a) the uncertainty from measurement noise, input variability, and environmental/operational variability in the training state, expressed through a single exceedance probability of change severity, and (b) the uncertainty from unknown environmental/operational conditions in the testing state, expressed through a range of possible values the exceedance probability may take. If the monitored system is fully instrumented, then the proposed DSF and health assessment method allows also an accurate element level change localization and severity estimation, while for partially instrumented systems it successfully identifies a region within which damage is confined. The proposed health assessment procedure is also applied to experimental data from a 4-story steel frame under base excitation on a shake table and is proved to be capable of identifying the location and severity of stiffness reduction with reasonable accuracy.

Acknowledgments

The authors acknowledge the financial support from Rutgers, Center for Advanced Infrastructure and Transportation - CAIT (Sponsor grant: DTRT12-G-UTC16). The authors also thank Adrian Brügger, Prof. Manolis Chatz is and Prof. Andrew Smyth for their collaboration and support during the experimental phase of the work.

References

Balsamo, L., Mukhopadhyay, S., Betti, R. and Lus, H. (2013a), "Damage detection using flexibility proportional coordinate modal assurance criterion", *Proceedings of the 31stIMAC*, Garden Grove, USA, February.

Balsamo, L., Mukhopadhyay, S., Betti, R. and Lus, H. (2013b), "Modal parameter based damage detection in operational modal analysis: A statistical pattern recognition approach", *Proceedings of the 11th International Conference on Structural Safety and Reliability*, New York, USA, June.

Balsamo, L., Betti, R. and Beigi, H.(2014), "A structural health monitoring strategy using cepstral features", *J. Sound Vib.*, **333**(19), 4526-4542.

Duan, Z., Yan, G., Ou, J. and Spencer, B.F. (2007), "Damage detection in ambient vibration using proportional flexibility matrix with incomplete measured DOFs", *Struct. Control. Health Monit.*, **14**(2), 186-196.

Farrar, C.R., Doebling, S. and Nix, D.A. (2001), "Vibration-based structural damage identification", *Philos. T. R. Soc. A*, **359**(1778), 131-149.

Farrar, C.R. and Worden, K. (2013), *Structural Health Monitoring: A Machine Learning Perspective*, John Wiley & Sons, Ltd., Chichester, UK.

Fraraccio, G., Brugger, A. and Betti, R. (2008), "Identification and damage detection in structures subjected to base excitation", *Exp. Mech.*, **48**(4), 521-528.

Friswell, M.I. (2007), "Damage identification using inverse methods", *Philos. T. R. Soc. A*, **365**, 393-410.

Hanselmann, A., Schrempf, O.C. and Hanebeck, U.D. (2007), "Optimal parametric density estimation by minimizing an analytic distance measure", *Proceedings of the 10th International Conference on Information Fusion*.

Hong, A.L., Ubertini, F. and Betti, R. (2013), "New stochastic subspace approach for system identification and its application to long-span bridges", *J. Eng. Mech. - ASCE*, **139**(6), 724-736.

Huang, Q., Gardoni, P. and Hurlebaus, S. (2012), "A probabilistic damage detection approach using vibration-based nondestructive testing", *Struct. Saf.*, **38**(2012), 11-21.

Katafygiotis, L.S. and Beck, J.L. (1998), "Updating models and their uncertainties. II: Model identifiability", *J. Eng. Mech. - ASCE*, **124**(4), 463-467.

Kim, J. and Stubbs, N. (2003), "Nondestructive crack detection algorithm for full-scale bridges", *J. Struct. Eng. - ASCE*, **129**(10), 1358-1366.

Lukaszyk, S. (2004), "A new concept of probability metric and its applications in approximation of scattered data sets", *Comput. Mech.*, **33**(4), 299-304.

Lus, H., Betti, R. and Longman, R.W. (1999), "Identification of linear structural systems using earthquake-induced vibration data", *Earthq. Eng. Struct. D.*, **28**, 1449-1467.

Mukhopadhyay, S., Lus, H., Hong, A.L. and Betti, R. (2012), "Propagation of mode shape errors in structural identification", *J. Sound Vib.*, **331**, 3961-3975.

Mukhopadhyay, S., Lus, H. and Betti, R. (2014a), "Modal parameter based structural identification using input-output data: Minimal instrumentation and global identifiability issues", *Mech. Syst. Signal Pr.*, **45**(2), 283-301.

Mukhopadhyay, S., Lus, H. and Betti, R. (2014b), "Structural identification with incomplete instrumentation and global identifiability requirements under base excitation", *Struct. Control. Health Monit.*, DOI: 10.1002/stc.1732.

Nayeri, R.D., Masri, S.F. and Chassiakos, A.G. (2007), "Application of structural health monitoring techniques to track structural changes in a retrofitted building based on ambient vibration", *J. Eng. Mech. - ASCE*, **133**(12), 1311-1325.

Sohn, H. (2007), "Effects of environmental and operational variability on structural health monitoring", *Philos. T. R. Soc. A*, **365**(1851), 539-560.

Soyoz, S. and Feng, M.Q. (2009), "Long-term monitoring and identification of bridge structural parameters", *Comput-Aided Civ. Inf.*, **24**(2), 82-92.

Yuen, K.V., Beck, J.L. and Katafygiotis, L.S. (2006), "Efficient model updating and health monitoring methodology using incomplete modal data without mode matching", *Struct. Control. Health Monit.*, **13**(1), 91-107.